Refractive Index of Spherical Waves in Magnetoplasma

Xueqin Huang[1] ***and Bodo W. Reinisch***[1,2]

[1] Center for Atmospheric Research, University of Massachusetts Lowell
600 Suffolk Street 3rd floor, Lowell, MA 01854 USA, Tel: +1 978-934-4900, Fax: +1 978-459-7915
Xueqin_Huang@uml.edu, Bodo.Reinisch@digisonde.com

[2] Lowell Digisonde International, LLC,
175 Cabot St, Lowell, MA 01854 USA, Tel: +1 978-735-4752, Fax: +1 978-735-4754

In geospace electromagnetic waves from a radio sounder travel in the ionosphere or the magnetosphere and, if reflected in the plasma, return to the receiver. The received signals provide the information of the sounded media. By analyzing the measured data physical parameters of the medium like density and movement can be obtained. The waves originate from a source of small dimensions relative to the distances involved and the resulting waves have spherical wave fronts. For ground-based sounding, when the wave reaches the ionosphere the radius of curvature is so large that the wave in a given direction can be treated as one of two plane waves, either L mode or R mode, and the error introduced with this approximation is generally believed to be negligibly small. For sounding in the topside ionosphere and the magnetosphere, however, the transmitter and receiver on board a rocket or satellite are located within an anisotropic medium, and the question arises how well the excited field is still approximated by a single plane wave in a given direction. An attempt is made in this paper to derive the properties of the excited electromagnetic field including the wave mode, polarization, and the spatial distribution of the power density when the current source is embedded in anisotropic plasma.

It is assumed that a sinusoidal steady current source is located in an unbounded uniform magneto-plasma described by the cold plasma theory, and that a sinusoidally varying electromagnetic field will be stimulated. The current source is arbitrary but confined to a limited region of space. When the z-axis is set along the direction of the ambient magnetic field and using the complex time factor $e^{j\omega t}$, the relative dielectric tensor, $\boldsymbol{\varepsilon}$, can be written in matrix form with the standard notation:

$$\boldsymbol{\varepsilon}=\begin{bmatrix}\varepsilon_1 & -j\varepsilon_2 & 0\\ j\varepsilon_2 & \varepsilon_1 & 0\\ 0 & 0 & \varepsilon_3\end{bmatrix},\quad \begin{cases}\varepsilon_1=1-\dfrac{XU}{U^2-Y^2},\ \varepsilon_2=\dfrac{XY}{U^2-Y^2},\ \varepsilon_3=1-\dfrac{X}{U}\\ X=\dfrac{{\omega_{pe}}^2}{\omega^2},\ \ Y=\dfrac{\omega_{ce}}{\omega},\ \ U=1-jZ,\ \ \mathrm{Z}=\dfrac{\nu}{\omega}\end{cases} \tag{1}$$

The radiation equation derived from the Maxwell equation system is analytically solved with the Green's function method for collisional magneto-plasma. The result for collisionless plasma is obtained as the limit of the general solution. The excited field can always be decomposed into two modes and, in the spherical coordinate system (r,α,β) with the origin at the current source center, the waves for each mode are expressed as a series of spherical waves whose amplitudes decrease as $1/r^i$ (i=1, 2, 3, …) by asymptotic expansion. For the far field only the1/r term is of importance:

$$\begin{aligned}\mathbf{E}(r,\alpha,\beta)&=\mathbf{E}_0(\alpha,\beta;\boldsymbol{\varepsilon})\frac{e^{-jk_0n_sr}}{r}\\ \mathbf{H}(r,\alpha,\beta)&=\mathbf{H}_0(\alpha,\beta;\boldsymbol{\varepsilon})\frac{e^{-jk_0n_sr}}{r}\end{aligned} \tag{2}$$

where $k_0=\omega/c$ is the wave number in free space. $\mathbf{E}_0(\alpha,\beta;\boldsymbol{\varepsilon})$ and $\mathbf{H}_0(\alpha,\beta;\boldsymbol{\varepsilon})$ depend on the distribution of the driving current source and the plasma parameters. The derived analytical solution is valid for any plasma parameters in the eight regions of the CMA diagram except for the cut off and resonance lines as the cold plasma theory cannot describe the phenomena for these region boarder lines (see Figure 1). In order to describe the phase variation with distance a spherical index n_s , i.e., a refractive index of spherical waves, is introduced:

$$n_s = n_z|\cos\alpha| + n_\rho \sin\alpha, \quad \left(-\frac{\pi}{2} \le \arg(n_s) \le 0\right)$$

$$n_z(n_\rho) = \left(\frac{2\varepsilon_1\varepsilon_3 - (\varepsilon_1+\varepsilon_3)n_\rho^{\ 2} + q_\pm(n_\rho)}{2\varepsilon_3}\right)^{1/2} \qquad (3)$$

$$q_\pm(n_\rho) = \left((\varepsilon_1-\varepsilon_3)^2 n_\rho^{\ 4} - 4\varepsilon_2^{\ 2}\varepsilon_3 n_\rho^{\ 2} + 4\varepsilon_2^{\ 2}\varepsilon_3^{\ 2}\right)^{1/2}, \quad \left(\mathrm{Re}(q_+) \ge 0,\ \mathrm{Re}(q_-) \le 0\right)$$

where $q_\pm$ serves as the discriminator of the two modes designated as "+" and "-" mode, respectively, and the values of n_ρ are the roots of the following equation:

$$n_\rho\left[-(\varepsilon_1+\varepsilon_3)q(n_\rho) + (\varepsilon_1-\varepsilon_3)^2 n_\rho^{\ 2} - 2\varepsilon_2^{\ 2}\varepsilon_3\right]|\cos\alpha| + 2\varepsilon_3 n_z(n_\rho)q(n_\rho)\sin\alpha = 0 \qquad (4)$$

For collisionless plasma the spherical refractive index becomes either pure real or pure imaginary indicating that the wave is either progressive or evanescent. The typical spherical indices for collisionless plasma are plotted in Figures 2a and 2b (solid lines) as a function of the polar angle from the direction of the ambient magnetic field (pointing to the top of the figure). The indices for plane waves are also plotted in the figure as dotted lines. Red color indicates that n_s is real, and green color that n_s is imaginary.

Similar to plane waves, the spherical refractive index surfaces are symmetrical with respect to the ambient magnetic field. For propagation parallel and perpendicular to the ambient magnetic field the spherical index is equal to the plane wave refractive index. In all other directions they are different. This difference is small for very weak plasma, but gets larger and larger with increasing anisotropy. The spherical wave with left-hand polarization (L-wave) is progressive in Regions 1, 2, and 3 and the index surface is continuously changing from one region to another. The spherical wave with right-hand polarization (R-wave) is progressive in Region 1 and becomes evanescent when crossing the cut-off line $X = 1 - Y$, but it appears again in the perpendicular directions in Region 3. In Region 4, only the R-wave is progressive and it becomes evanescent when crossing the cut-off line $X = 1 + Y$. In Region 5, the two mode waves are evanescent, indicating that the current source cannot excite any progressive waves in this region. In Region 6 the two wave modes are progressive, but the index surfaces do not change continuously when crossing the region boarder lines. In Regions 7 and 8, the whistler wave (R-wave) is excited and is progressive in a limited range of directions referred to as the radiation cone. The angle of the radiation cone is complementary to the angle of the resonance cone as defined for plane waves. In Region 7, the progressive L-wave is also excited and becomes evanescent when crossing the cut-off line $X = 1 + Y$.

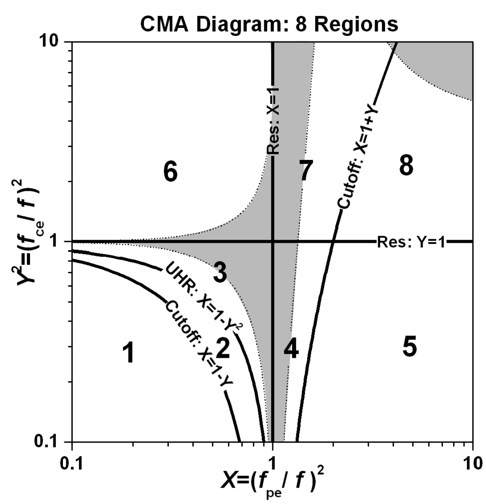

Figure 1. CMA diagram for cold plasma.

In the shaded areas in Figure 1 two or three sub-mode spherical waves are excited in a given direction, they have the same polarization but different refractive indices. The spherical indices for the sub-modes were not plotted in Figure 2.

For excited spherical waves the time-averaged energy flow is in the radial direction parallel to the wave normal. This is different from the plane wave description in an anisotropic medium where the wave normal and the energy flow are in different directions making the problem more complicated than the isotropic case. The directional agreement of the phase and group velocities of the excited spherical waves makes the anisotropic plasma look like an isotropic medium except that the refractive index changes with the angle from the ambient magnetic field.

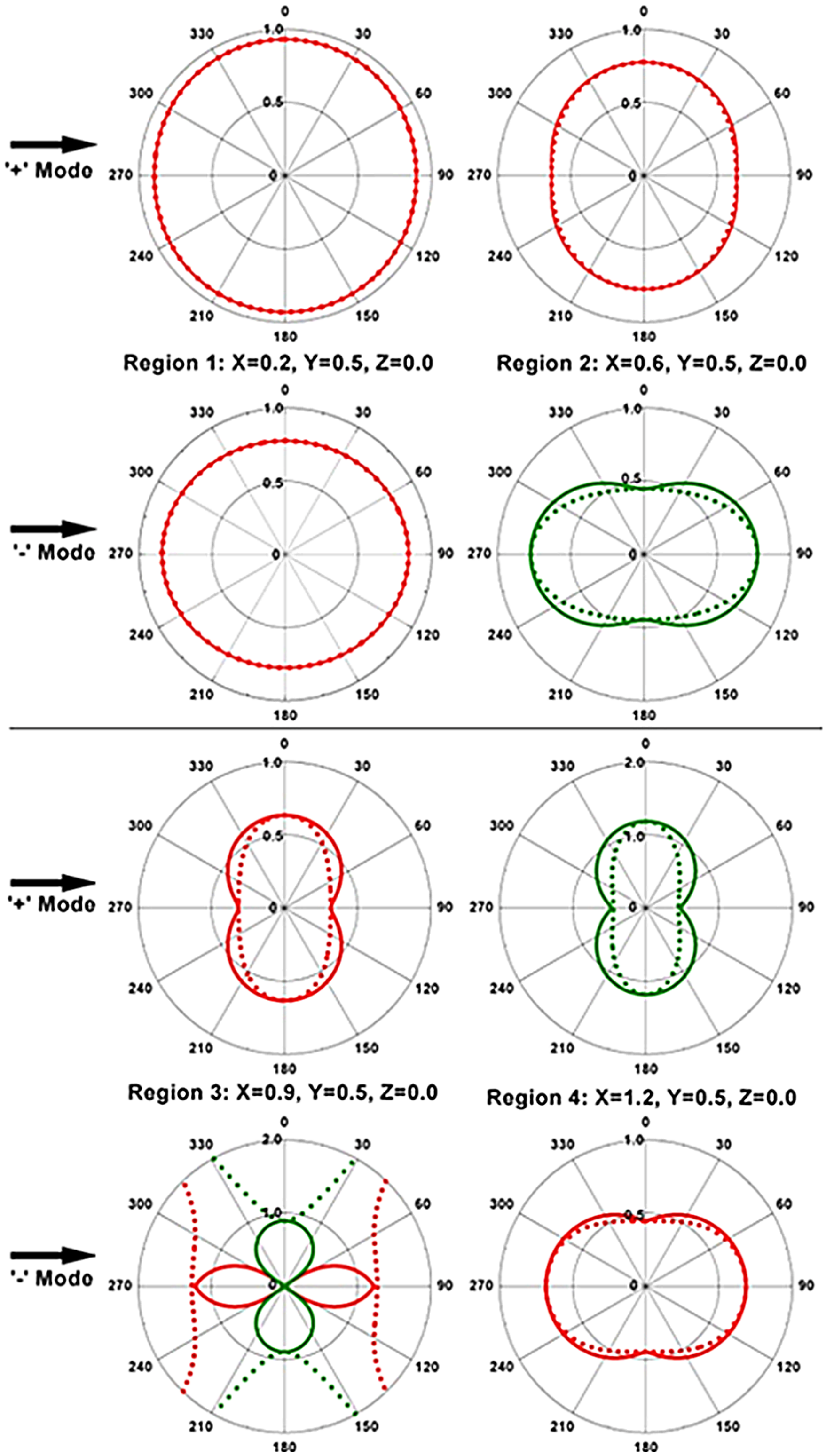

Figure 2a. Spherical and plane wave refractive indices for collisionless plasma for CMA Regions 1 to 4 (red = real, green = imaginary)

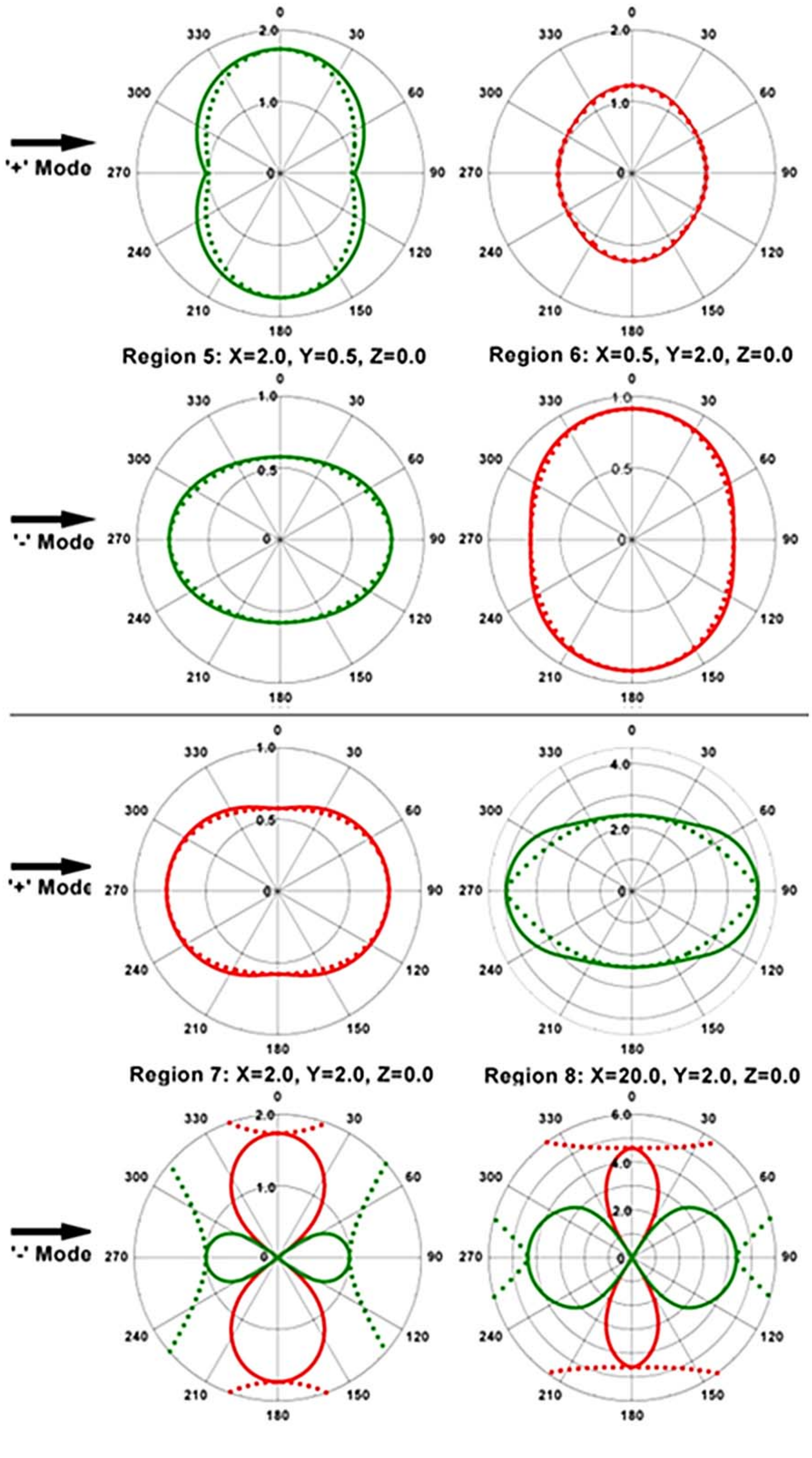

Figure 2b. Same as 2a but for CMA Regions 5 to 8.